

MODELING OF THERMO-HYDRODYNAMIC-CHEMICAL PROCESSES: SOME APPLICATIONS TO ACTIVE HYDROTHERMAL SYSTEMS

Alexey Kiryukhin^{#&}, Tianfu Xu[#], Karsten Pruess[#], Igor Slotvsov[&]

[#] - Lawrence Berkeley National Laboratory, MS90-1116, Berkeley CA 94720, USA

[&] - Institute of Volcanology, Piip-9, Petropavlovsk-Kamchatsky 683006, Russia

e-mail: AVKiryukhin@lbl.gov

ABSTRACT

Available data on secondary mineral distributions, host rock properties and chemical composition of deep geothermal fluids ("parent geothermal fluids") of nine geothermal fields: Mutnovsky, Pauzhetsky (Kamchatka), Sumikawa, Kakkonda, Uenotai, Okuaizu, Hachijo-jima, Ogiri, Fushime (Japan) were used for thermo-hydrodynamic-chemical (THC) models calibration study. THC processes in hydrothermal systems were modeled with the TOUGHREACT numerical code (Xu and Pruess, 2001). Steady-state flow and single-phase liquid conditions were assumed. Our initial studies assume a highly simplified geochemical system, which includes the following mineral phases: quartz, K-feldspar, Na-feldspar, and cristobalite. Fluid containing Cl⁻, Na⁺ and CO₂ was recharged to geothermal reservoirs under a specified range (10-200°C) of temperatures. Based on the modeling the following results were obtained: (1) Model validation by Na-K and SiO₂ geothermometers; (2) Precipitation (K-feldspar and quartz) dominates over dissolution (Na-feldspar), meaning that *selfsealing of reservoir* took place. This has been confirmed by K-feldspar abundance in production zones at the geothermal fields; (3) Model sensitivity of mineral phase change to pH, porosity and flowrate has been studied.

INTRODUCTION

Modeling thermal-hydrodynamic-chemical (THC) processes in active hydrothermal systems is a key issue for THC model calibration and proper design of underground nuclear waste repository sites, understanding the formation of ore deposits, as well as for different geothermal applications. Following are brief descriptions of the nine Kamchatka and Japanese geothermal fields currently found useful for THC model calibration study.

Mutnovsky geothermal field (Dachny site) Kamchatka, Russia (Kiryukhin, 1993, 1996, Slotvsov, 1999). The 80 m-thickness planar-type production zone has north-east-north strike and 60° south-east-south dip. High temperature liquid fluid

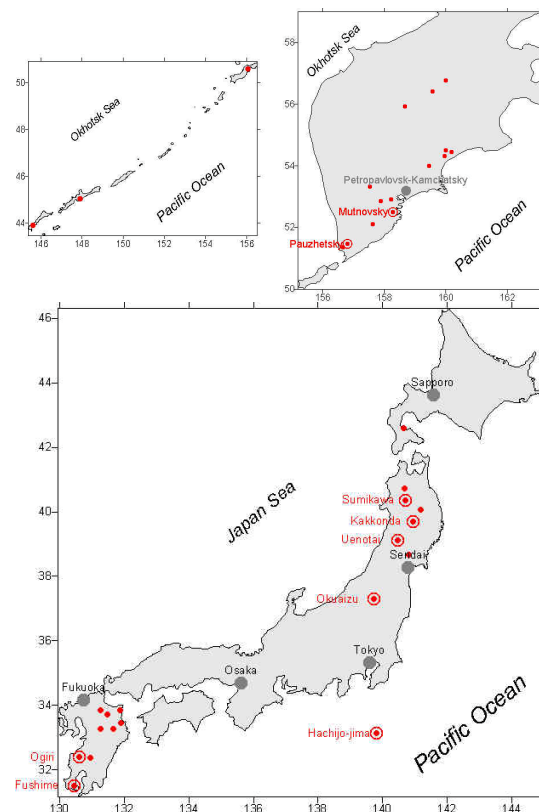


Fig.1 Geothermal fields of Kamchatka, Kurile Islands and Japan – circles, currently found useful for THC (thermal-hydrodynamic-chemical) studies - double circles.

(40 kg/s, 1390 kJ/kg) upflows from south-east of the fracture, where a deep 280°C liquid-dominated zone shows quartz-epidote-chlorite secondary hydrothermal mineralization. In the upper part of "Main" production zone ascending fluids encounter two-phase conditions characterized by prehnite-wairakite precipitation. Fracture host rocks are: diorites, Miocene-Pliocene sandstones, rhyolite and andesite tuffs and lavas. Shallow steam condensate and meteoric water mixing zone is characterized by calcite-chlorite-illite mineralization.

Pauzhetsky geothermal field, Kamchatka, Russia (Sugrovov, Belousov (1965), Naboko, 1963). Sub-

lateral liquid flow at temperatures of 180-200°C occurs at depth 100 - 800 m within the high permeability Neogene-Quaternary psephytic tuffs. The dominant secondary minerals in production zone are zeolites (mostly laumontite), feldspars, carbonates and chlorites. Feldspars form at 160-190°C as an albite and adularia, associated with laumontite and calcite. K-feldspar (adularia) occurs in upper high temperature zone, while Na-feldspar (albite) is present in lower (temperature inversion) zones.

Sumikawa geothermal field, Japan (Ariki, 1999). The reservoir consists of dacitic pyroclastic rocks, marine sedimentary units, altered andesite, and a granitic body intruded into the Tertiary formations. A production zone in two-phase conditions with temperatures up to 300°C is traced by zeolites (wairakite), while epidote and chlorite are observed, too. Planar fracture control of this field (west-east strike, south dip 40-50°) is possible.

Kakkonda geothermal field, Japan (Muraoka, et al, 1998). A neo-granitic pluton (0.19 Ma) found beneath this geothermal field acts as a magmatic heat source for the geothermal system. The reservoir is composed mainly of Miocene andesitic and dacitic tuffs. Production zones under liquid conditions and temperatures 220-260 °C (shallow reservoir) and 280-340°C (deep reservoir) are traced by epidote, anhydrite, sericite, prehnite. Abundant secondary minerals are quartz, chlorite, calcite and Ca-feldspar plagioclase. Secondary K-feldspar is found too, while Na-feldspar is absent. There were at least four heating events in the history of this field, which resulted in a very complicated superposition of secondary mineralization. An inflection point in the temperature profile of super-deep well WD-1a occurs at a depth of 3100 m and a temperature of 380°C, and marks the expected brittle-plastic boundary and the maximum depth of hydrothermal convection. A two-phase zone of Na-Cl brine and non-condensable gas (CO₂, H₂S) exists as intra-crystalline fluid below the hydrothermal convection system.

Uenotai geothermal field, Japan (Naka et al, 1992, Takeno,2000). The reservoir consists of Miocene andesite and pre-Tertiary granite. Central zone of 300°C reservoir is boiling and surrounding liquid-dominant zone. Production zones are traced by secondary quartz, epidote, calcite and zeolites (wairakite); while other zeolites (laumontite, mordenite) are found outside of production zones.

Okuaizu geothermal field, Japan (Nitta, et al, 1995, Mizugaki, 2000). The principal production zone occurs at a depth of 1.0-2.6 km within fractured Neogene “green tuff” formations (subaqueous volcanic rocks, that have been altered to a green color) along two northwest-trending faults to the southeast of the caldera: Chinokezawa and

Sarukurazawa. High salinity Na-Cl (about 5-15 g/kg) and gas enriched (CO₂, 10 – 80 g/kg) geothermal fluid circulation is characterized by calcite, anhydrite, chlorite and sericite occurrence at 250-300°C. A shallow reservoir is traced by K-feldspar. The upper part of production zone is sealed mainly by smectite and mordenite.

Hachijo-jima geothermal field, Japan (Matsuyama, et al, 2000). The high-temperature liquid dominated system exists in fractures of the Tertiary andesite and basalt formation. These fractures serve as conduits for the ascent of geothermal fluid, and act as a geothermal reservoir. Secondary minerals distributed in the upper part of 300 °C upflow in fractured andesitic Tertiary rocks are: quartz, calcite and anhydrite. Production zones are traced by wairakite.

Ogiri geothermal field, Japan (Goko, 2000). This is the Ginyu fault system (70-75°E strike, 63-72°N dip, width of 20 m) of a uniform liquid 232°C reservoir in andesite host rocks. There is no indication of superposition or retrograde hydrothermal alteration. The distribution of hydrothermal minerals is distinctly parallel to the isothermal contours. Wairakite and chlorite-smectite indicate the proximity to the Ginyu fault, and whether or not a well has been drilled completely through the fault zone. K-feldspar, chlorite and epidote are also present in the production zone. The shallow impermeable zone, produced by self-sealing through the formation of smectite, has a 200-400 m vertical extent and overlies the Ginyu fault like an umbrella, acting as a cap rock.

Fushime geothermal field, Japan (Okada et al, 2000). The main reservoir is composed of andesitic-dacitic lavas and tuffs in fractured zones developed around a dacite intrusion. One is a NNE-SSW trending zone to the west, and the other is a NW-SE trending zone to the south. In the main production zone temperatures exceed 300°C at a depth of 1700 m below sea level. The Cl, Br/Cl ratios and stable isotope data indicate that the Fushime geothermal fluid originated from CO₂ enriched (up to 12.5 g/kg in steam phase) heated sea water ascending in single- phase conditions. The production zones are usually located in the chlorite and epidote zones. K- feldspar is abundant in the center of the feed points of the production wells, while albite-chlorite is found in the outermost portion of the hydrothermal reservoir.

Based on the above examples of geothermal fields following gas and chemistry data of fluids and secondary minerals are expected to be main contributors to selfsealing and precipitation processes in hydrothermal systems at temperatures below 350°C (Table 1, Fig.2).

Table 1. Gas and fluid chemistry data of selected geothermal fields (mg/kg), referred to deep reservoir conditions (“parent geothermal fluids”). Note: pH data – laboratory values of brines.

Geothermal filed	pH	Na ⁺	K ⁺	Ca ⁺⁺	Cl ⁻	SO ₄ ⁻⁻
Mutnovsky	7.9	156.6	29.6	1.3	185.1	80.3
Pauzhetsky	8.5	580.6	46.1	38.6	955.6	85.6
Sumikawa	7.6	181.6	30.5	2.9	248.1	51.9
Kakkonda		375.0			570.0	
Uenotai	9.5	110.5	22.2	0.2	143.6	1.3
Okuazu	6.6	5202	1451	769	11100	5.0
Hachijo-jima	6.2	8290	464	1020	14400	479.0
Ogiri	8.7	441	53.4	11.0	596.0	198.0
Fushime	6.9	8943	2082	1668	18086	27.4

Table 1. (continued)

Geothermal filed	HCO ₃ ⁻	SiO ₂	CO ₂	H ₂ S	Water recharge
Mutnovsky	53.9	682.7	13.2	3.2	Meteoric
Pauzhetsky	7.9	167.0	CO2	N2	Meteoric
Sumikawa	35.5	435.9	69.8	17.4	Meteoric
Kakkonda			1.0		Meteoric
Uenotai		487.1	1934	484	Meteoric
Okuazu		733.0	32800	700	Meteoric
Hachijo-jima	18.7	918.0	30000	7300	Sea+ meteoric
Ogiri	16.0	628.0	10.0	2.6	Meteoric
Fushime		397.1	4158	123.1	Sea

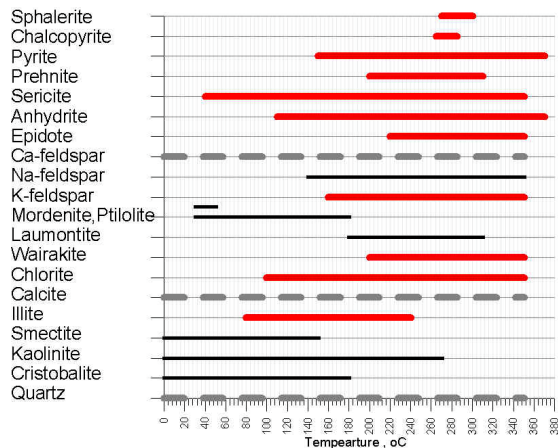


Fig.2. Secondary minerals in geothermal fields of Kamchatka and Japan as a function of temperature and type of permeability: **thick lines** – reservoir, **thin lines** – caprock, **dashed lines** - caprock + reservoir

MODEL SETUP

The current conceptual understanding of THC processes in hydrothermal systems may be expressed as (Fig.3). Cold meteoric water from a recharge area descends through sub-vertical channels, such as permeable faults or sub-vertical intrusive body contacts, to a deep heat exchange high-temperature zone. Cold meteoric water converts to high temperature NaCl and CO₂ enriched “parent geothermal fluid” through heat and chemical exchange. Basically, the “parent geothermal fluid” of geothermal systems has two components: meteoric water and magmatic fluid. Deep level magmatic fluid contributes HCl, HF, SO₂, H₂O, CO₂, H₂S gases which convert to dominant NaCl-CO₂ form due to interaction with host magmatic rocks. These fluids may in part become trapped below brittle/plastic boundaries of intrusions in the form of quartz polyphase NaCl - CO₂ inclusions (as proved by deep drilling in Kakkonda geothermal field, Muraoka et al, 1998). Then fluids ascend through high- permeability zones (“geothermal reservoirs”), and finally discharge at the earth surface in the form of hot springs and fumaroles. Flows from recharge to discharge areas are driven by pressure and fluid density differences (forced and free convection).

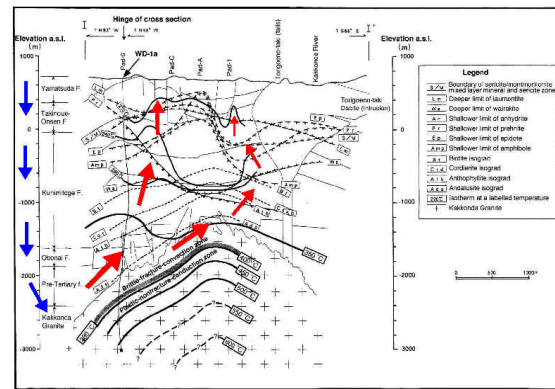


Fig. 3. Conceptual model of the THC processes in hydrothermal system based on the example of Kakkonda geothermal field (Muraoka et al, 1998). Suggested circulation patterns: downward arrows – meteoric recharge, upward arrows - ascending high temperature geothermal fluids

A simplified conceptual model of hydrothermal systems may be expressed as connected model elements B 1, R-elements and D 1 (Fig.4). B 1 is a basement element, where “parent geothermal fluid” originates. R-elements - are subsequent connected reservoir elements, where “parent geothermal fluid” ascends through specified temperature steps. D 1 is a discharge element assigned with constant atmospheric pressure and surface temperature conditions (1 bar, 10°C). Temperatures in all

elements are kept constant by specifying artificially high densities (10^{+15} kg/m³) in all elements of the model, and steady state fluid flow through the system was specified to simplify reactive chemical transport considerations. The TOUGHREACT code was used in this work (Xu and Pruess, 2001 a,b)

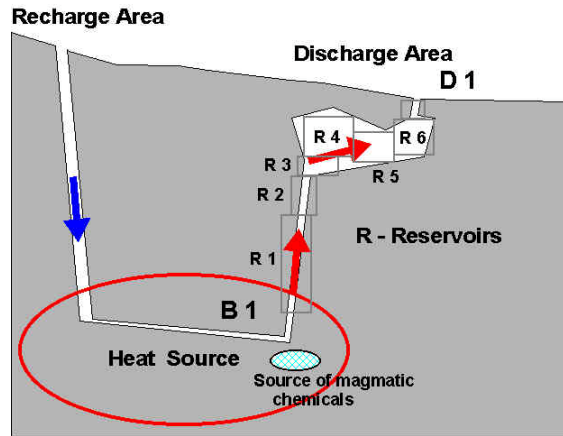


Fig.4 Conceptual model of a hydrothermal system superposed by numerical grid of a “lumped parameter pipe model”.

A test problem was designed to study the long-term chemical interaction of the “parent geothermal fluid” along fluid upflow under specified temperature conditions in the range of temperatures from 10 to 200°C. Initial chemical composition of fluids was assumed meteoric (R-elements), while “parent fluid” composition was assumed in B 1 (Table 2).

Table 2. Total concentrations of the fluid species, used in the model (mg/kg H₂O)

Fluid	pH	Na	K	Al
Meteoric	6.9	44	3	2
Parent geothermal	5.6	4460	570	0

Table 2. (continued)

Fluid	Cl	SO ₄	SiO ₂	CO ₂
Meteoric	6	0	249	44
Parent geothermal	7650	0	248	9090

Initial mineral composition of intrusion and geothermal reservoir rocks was specified as granodiorite (or dacite) composition (49 % low-albite NaAlSi₃O₈, 24% microcline KAlSi₃O₈, 27% -quartz SiO₂). The geochemical system also includes cristobalite. The following form of rate law used: rate = k S exp(E_a/(R*298.15)-E_a/(RT)), where k- chemical dissolution/precipitation kinetic rate constant at 25°C, mol/s m², S - surface area,m²/dm³, and E_a-activation

energy, kJ/kmol used for modeling of kinetically controlled mineral dissolution and precipitation (Table 3). The total surface area of chemical interaction was assumed to be shared between minerals according to volume fractions, except for cristobalite, which was assumed to be 0.001 m²/dm³ (Table 3).

Table 3 Kinetic parameters for chemical interaction.

Minerals	k mol/s m ²	S m ² /dm ³	E _a kJ/mol
Quartz	4.300E-14	0.027	75.0
Cristobalite	3.1623e-13	0.001	69.08
K-feldspar microcline	1.0000e-12	0.024	67.83
Na-feldspar low-albite	1.0000e-12	0.0489	67.83

RESULTS AND DISCUSSION

“Parent geothermal fluid “ (pH=5.6, Cl-Na (12.9 g/kg), CO₂ enriched (9.1 g/kg)) was recharged to the model geothermal reservoirs under a specified range (10-200°C) of temperatures during 100,000 years. It was found that convergence criteria (relative tolerance of concentrations for whole system) ≤10⁻⁶ and time steps ≤10 years were sufficient for geochemical problem convergence. Study of the grid sensitivity of the model (6-element vs. 20-element grid) shows reasonable convergence, and a 20-element regular grid was used for the following study. Chemical characteristics of reservoir fluids are stabilized after 1000 years and reasonably match known geothermal systems.

Na-K and SiO₂ geothermometers validation of the model

Na-K geothermometer (Arnorsson, 1999, Apps, 2001) reasonably matches corresponding reservoir temperatures in the range of 60 - 200°C for evolution test (Fig.5). Apps Na-K geothermometer is based on the same thermodynamic data as used by TOUGHREACT and yields absolute error less than 4°C. SiO₂ geothermometer (Fournier, 1981) shows significant deviations from the model, while Apps (2002) SiO₂ geothermometer (based on the same thermodynamic data as used by TOUGHREACT) agrees better in the range of temperatures 60 - 200 °C for evolution test (absolute error less than +5 °C, Fig.6). Over-estimations for both geothermometers (Na-K and SiO₂) at lower temperatures (less than 60°C) may be caused by up-stream supersaturation kinetic effects due to high-temperature elements below. This means that conditions are closed to chemical equilibrium along ascending flow in the temperature range 60-200°C.

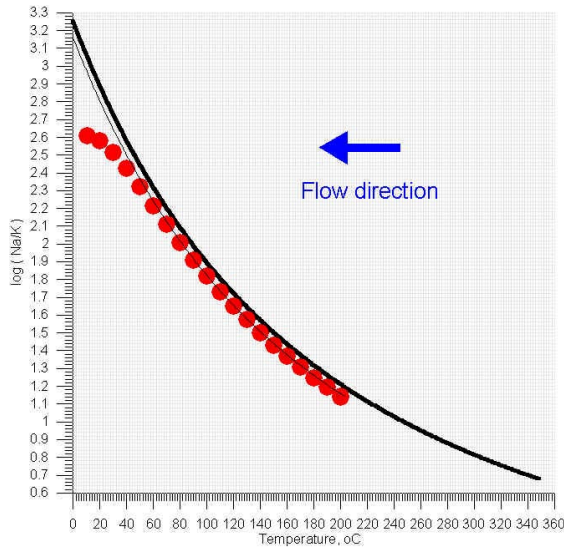


Fig.5. Na-K geothermometer match: Na-K geothermometer (Arnorsson, 1999) – thick line, Na-K geothermometer (Apps, pers.com.,2001) – thin line, TOUGHREACT data at R- elements at modeling time 100,000 years – circles.

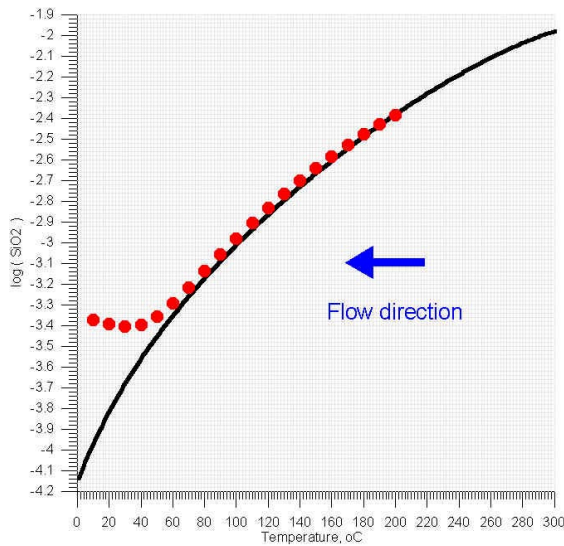


Fig.6. SiO₂ geothermometer match: SiO₂ geothermometer (Apps, pers.com.,2002) – thick line, TOUGHREACT data – circles.

Change of mineral phases along ascending fluid flow

Fig.7 shows an example of the chemical evolution in reservoir element R5 (160°C) of the model during 100,000 years. Distribution of change of the mineral phase along ascending fluid stream by 100,000 year are: Na-Feldspar (albite) dissolution (up to -12.6%) and K-feldspar (microcline) precipitation (up to 13.7%), significant quartz precipitation (up to 0.8%) was found too (Fig. 7). Precipitation dominates over dissolution, which means that selfsealing of reservoir took place by K-feldspar and quartz deposition.

Secondary K-feldspar abundance in production zones was confirmed by observations at the following geothermal fields: Ogiri, Kakkonda, Okuaizo, Fushime (Japan), Pauzhetsky (Russia), while secondary Na-feldspar was not found in main production zones.

Although it was suggested that additional HCl input to the system may accelerate fluid-rock interaction processes, the model showed no significant influence of pH (in the range of 3.1 – 5.6) on mineral dissolution/precipitation rates.

The basic value of porosity assigned was 0.1, while additional scenarios considered porosity values of 0.03 and 0.5. The model showed no significant influence of porosity on mineral dissolution/precipitation.

The basic value of permeability assigned was 100 mD, which corresponds to steady state up-flow rate 30.3 kg/s. Two additional scenarios were analyzed in the model with permeabilities of 10 mD (flowrate 3.0 kg/s), and 300 mD (flowrate 90.9 kg/s). Significant influence of flowrate on mineral phase change along ascending flow is shown in Figs. 8, 9, 10 and 11. Increase of flowrates corresponds to increase of precipitation, which may reach 4.8 % in total volume change of mineral phase at 140-150°C (Fig. 11). A possible interpretation is that larger flowrates correspond to larger K⁺ recharge inflows through the system, that serve as the main source of K-feldspar precipitation.

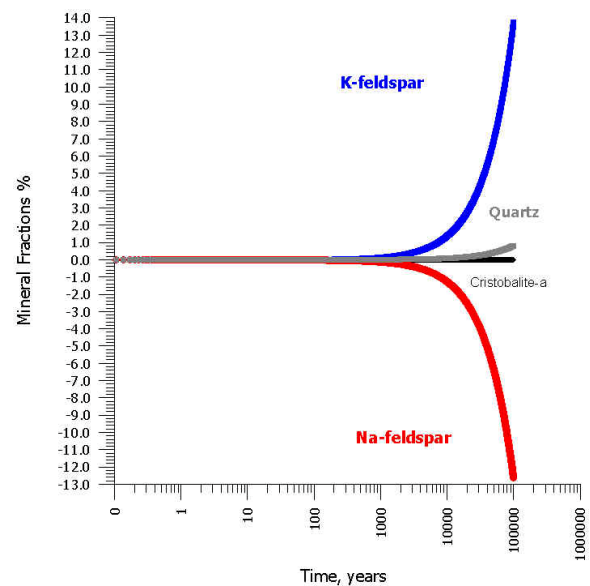


Fig. 7 Chemical evolution of mineral phases - changes of volume fractions % in liquid dominated reservoir (R5, 160°C), time step $\Delta t = 10$ years.

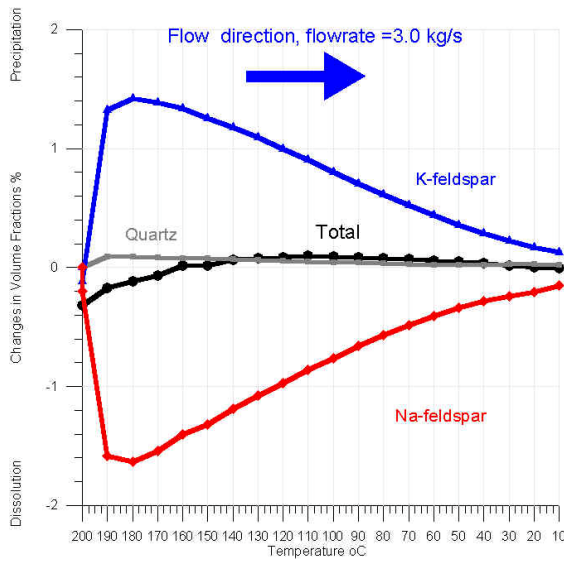


Fig. 8 Chemical evolution of mineral phases - changes of volume fractions % in liquid dominated reservoir along ascending up-flow in temperature range 10-200 °C (R-elements) after 100,000 years (flowrate = 3.0 kg/s).

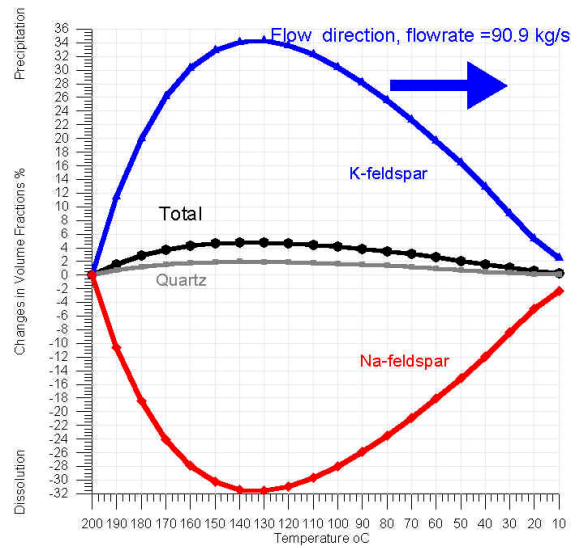


Fig. 10 Chemical evolution of mineral phases - changes of volume fractions % in liquid dominated reservoir along ascending up-flow in temperature range 10-200 °C (R- elements) after 100,000 years (flowrate = 90.9 kg/s)

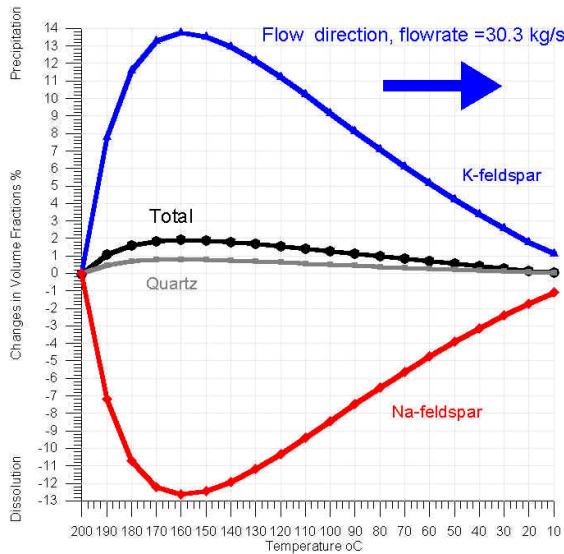


Fig. 9 Chemical evolution of mineral phases - changes of volume fractions % in liquid dominated reservoir along ascending up-flow in temperature range 10-200 °C (R-elements) after 100,000 years (flowrate = 30.3 kg/s).

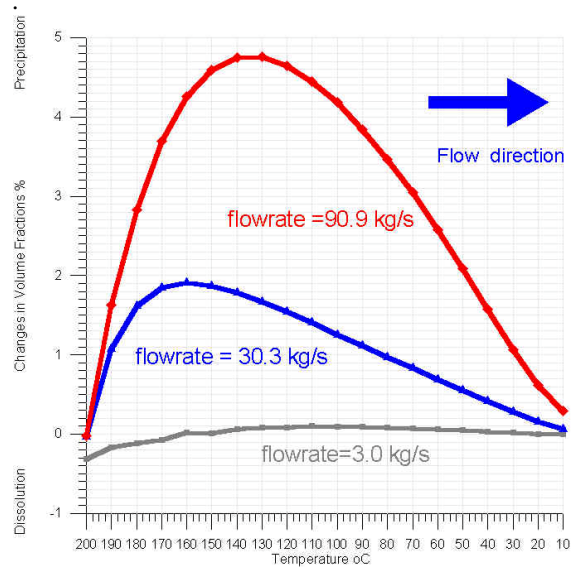


Fig. 11 Model sensitivity to permeability-flowrate change. Total mineral phase changes (in volume fractions %) along ascending up-flow in temperature range 10-200 °C (R- elements) after 100,000 years vs. flowrates (3.0, 30.3, 90.9 kg/s).

CONCLUSIONS

1. Available data on secondary mineral distributions, host rock properties and chemical composition of deep geothermal fluids ("parent geothermal fluids") of nine geothermal fields: Mutnovsky, Pauzhetsky (Kamchatka), Sumikawa, Kakkonda, Uenotai, Okuaizu, Hachijo-jima, Ogiri, Fushime (Japan) have been used for THC model calibration study. Chemical evolution of hydrothermal system above granodiorite intrusion was modeled with TOUGHREACT. Steady-state flow and single-phase liquid conditions were assumed. Our initial studies assume a highly simplified geochemical system, which includes the following mineral phases: quartz, K-feldspar, Na-feldspar, and cristobalite. Cl-Na CO₂ enriched fluid was recharged to geothermal reservoirs maintained under specified range (10-200°C) of temperatures.

2. Model validation of geothermometers : Na-K and SiO₂ geothermometers, based on TOUGHREACT thermodynamic data base (Apps, 2001, 2002), reasonably match corresponding reservoir temperatures in the range of 60 - 200°C, indicating conditions close to chemical equilibrium along ascending fluid flow in this temperatures range. Over-estimations for both geothermometers (Na-K and SiO₂) at low temperatures (less than 60°C) are caused by up-stream supersaturation kinetic effects due to high-temperature elements below.

3. Modeling chemical evolution above granodiorite intrusion shows the following changes of mineral phase along fluid up-flow during 100,000 year time period: Na-Feldspar (albite) dissolution (up to - 12.6% at 160°C), K-feldspar (microcline) precipitation (up to 13.7% at 160 °C) and quartz precipitation (up to 0.8% at 160 °C). Precipitation dominating over dissolution means that *porosity reduction of reservoir* took place due to K-feldspar and quartz deposition. K-feldspar abundance in production zones was confirmed at the following geothermal fields: Ogiri, Kakkonda, Okuaizu, Fushime (Japan), Pauzhetsky (Russia), while Na-feldspar was absent.

4. Model sensitivity of mineral phase change to pH values of parent fluids (pH of 3.1-5.6) and porosity (0.03 - 0.50) was not found significant. Study of the model sensitivity to flowrate (3.0 - 90.9 kg/s) shows that increase of flowrates corresponds to increase of precipitation, which may reach 4.8 % in total volume change of mineral phase at 140-150°C. Possible interpretations is that larger flowrates correspond to larger K⁺ recharge through the system, that may serve as the main source of K-feldspar precipitation due to Na-K temperature buffer of the fluid system. Larger

specific volume of K-feldspar compare to Na-feldspar (8%) may facilitate selfsealing processes.

5. Further developments and improvements of the THC model of active hydrothermal systems are underway and include the following items: extension of modeling temperature range, introduction of different type of host rocks; consideration of clay minerals (smectites, illites, kaolinites), Ca-feldspar, zeolites and other mineral phases; consideration of additional species in gas and liquid phases (HCl, H₂S, Ca⁺⁺, Mg⁺⁺, SO₄⁻); investigation of boiling and condensation effects on mineral precipitation and dissolution; more detailed representation of reservoir geometry and fracture-matrix interactions; and coupling between chemical evolution and fluid flow through changes in porosity and permeability.

ACKNOWLEDGEMENTS

The authors express their gratitude for helpful discussion to G. Bodvarsson, A. Symmons, J. Apps, A. Truesdell, V. Belousov, S. Flexser, M. Lippmann, E. Sonnenthal, N. Spycher, K. Williamson, P. Kruger, P. Dobson, N. Tsuchiya, L. Richard and E. Kalacheva. This work was supported by the Assistant Secretary for Energy Efficiency and Renewable Energy, Office of Power Technologies, Office of Wind and Geothermal Technologies, of the U.S. Department of Energy under contract No. DE-AC03-76SF00098.

REFERENCES

1. J.Apps, 2001, pers.com.
2. J.Apps, 2002, pers.com.
3. S. Arnorsson, A. Stefansson (1999) Assessment of feldspar solubility constants in water in the range 0°C to 350°C at vapor saturation pressures // American Journal of Sciences, Vol.299, p. 176-209.
4. K. Arika, H. Kato, A. Ueda, M. Bamba (2000) Characteristics and Management of the Sumikawa Geothermal Reservoir, Northeastern Japan // Geothermics, v.29, p.171-189.
5. Aumento F. (1985) Conceptual Models of the Circulation of Geothermal Fluids Derived from Alteration Mineralogical Data // Geothermal Resources Council, Transactions, Vol.9, part 2, p.383 - 387.
6. Fournier R.O. (1981) Application of water geochemistry to geothermal exploration and reservoir engineering // Geothermal Systems: Principles and Case Histories, N.Y.: Pergamon Press, p.109-140.

7. K.Goko (2000) Structure and hydrology of the Ogiri field, West Kirishima geothermal area, Kyushu, Japan // *Geothermics*, v.29, N.2, p.127-149.
8. Kiryukhin A.V. (2001) Geothermal Energy Transport in Recent Volcanism Areas (Kamchatka and Kurile Islands): Conceptual Model and Some Examples // 26-th Workshop on Geothermal Res. Eng., Stanford, CA, January 29-31
9. Kiryukhin A.V. (1993) High temperature fluid flows in the Mutnovsky hydrothermal system, Kamchatka // *Geothermics*, v.23, N 1, p. 49-64.
10. Kiryukhin A.V. (1996) Modeling Studies: the Dachny Geothermal Reservoir, Kamchatka, Russia // *Geothermics*, Vol.25, No.1, p. 63-90.
11. K.Matsuyama, N. Narita, K. Tomita, T. Majima (2000) // Geothermal resources of Hachijojima // *Geothermics* v.29, p. 213-232
12. K.Mizugaki (2000) Geologic structure and volcanic history of the Yanaizu-Nishiyama (Okuaizu) geothermal field, Northeast Japan // *Geothermics* 29, p. 233-256
13. H. Muraoka, T. Uchida, M. Sasada, M. Yagi, K. Akaku, M. Sasaki, K. Yasukawa, S. Miyazaki, N. Doi, S. Saito, K. Sato, S. Tanaka (1998) Deep Geothermal Resources Survey Program: Igneous, Metamorphic and Hydrothermal Processes in a Well Encountering 500°C at 3729 m Depth, Kakkonda, Japan // *Geothermics* Vol. 27, No. 5/6, pp. 507-534
14. Naboko S.I. (1963) Hydrothermal Metamorphism in Volcanic Areas // USSR AS Publishers, Moscow, 172 p.
15. Naka T., Okada H. (1992) Exploration and development of Uenotai geothermal field, Akita prefecture, northeastern Japan. *Resource Geology* 42, 223-240 (in Japanese with English abstract).
16. Nakamura H., Sumi K. (1981) Exploration and development at Takinoe, Japan // *Geothermal Systems: Principles and Case Histories*, NY Pergamon Press, p. 248-272.
17. Nitta T., Tsukagoshi S., Adachi M., Seo K. (1995) Exploration and development in the Okuaizu geothermal field Japan (In Japanese with English abstract), *Resource Geol* 45, 201-212.
18. H.Okada, Y. Yasuda, M. Yagi, K. Kai (2000) Geology and fluid chemistry of the Fushime geothermal field, Kyushu, Japan // *Geothermics* 29, 279-311
19. Sugrobov V.M., Belousov V.M., et al *Pauzhetka Thermal Waters in Kamchatka (1965)* // Moscow, Nauka Publ., 205 p.
20. Slovtsov I.B. (1999) (personal communication)
21. N. Takeno (2000) Thermal and geochemical structure of the Uenotai geothermal system, Japan // *Geothermics* 29, p. 257- 277
22. Ueda A., Kubota Y., Katoh H., Hatakeyama K., Matsubaya O. (1991) Geochemical characteristics of the Sumikawa geothermal system, northeast Japan. *Geochemical Journal* 25, 223-244.
23. T.Xu and K.Pruess (2001a) On Fluid Flow and Mineral Alteration in Fractured Caprock of Magmatic Hydrothermal Systems// *Journal of Geophysical Research*, Vol.106, No.B2, p.2121-2138.
24. Xu, T. and K. Pruess (2001b). Modeling Multiphase Non-isothermal Fluid Flow and Reactive Geochemical Transport in Variably Saturated Fractured Rocks: 1.Methodology, *American Journal of Science*, Vol. 301, pp. 16-33.